https://doi.org/10.5194/essd-2025-8
Preprint. Discussion started: 17 February 2025

Open Access Earth System Science Data Discussions

Science data collection by the New Zealand Defence Force during the 2022 Antarctic Resupply Mission

Sally Garrett[1], Peter McComb[2], John Harris[1], Ursula Crabtree[2]

[1]Defence Science + Technology, New Zealand Defence Force, Auckland, 0654, New Zealand
[2]Oceanum Limited, New Plymouth, New Zealand

Correspondence to: Sally Garrett (sally.garrett@nzdf.mil.nz)

Abstract. The maiden resupply voyage of HMNZS AOTEAROA to Winter Quarters Bay, McMurdo Sound, provided a vessel of opportunity to complete experimentation in the Ross Sea and Southern Ocean, focussed on improving maritime safety. The science programs on the voyage included the deployment of 21 free floating wave buoys, 10 Global Drifters, 2 Argo Floats and 85 expendable bathythermograph profilers. In addition, measurements of meteorological and oceanographic conditions and sea ice characteristics were captured from onboard the ship and augmented with satellite-based synthetic aperture radar captures and high-resolution wave modelling. An aligned experiment was also undertaken to assess the performance of Global Navigation Satellite Systems at high latitudes. The full set of voyage data and instructions for their access are described.

1 Introduction

The New Zealand Defence Force has a long-standing commitment to supporting Antarctica New Zealand and international scientific and environmental programmes on the ice in Antarctica. Since the 1970s, however, logistics support, including resupply of freight and people, has only been completed via Royal New Zealand Air Force C-130 Hercules and Boeing 757 aircraft. In 2020, the Royal New Zealand Navy commissioned HMNZS AOTEAROA, a purpose-built, polar-class sustainment vessel specifically designed to resupply Antarctic bases once again. The ship can operate deep into the Southern Ocean and the Ross Sea, with an ice-strengthened hull and upper deck trace heating.

In February 2022, HMNZS AOTEAROA completed her maiden resupply voyage to Winter Quarters Bay, McMurdo Sound. The ship departed Lyttleton on February 3, 2022, and returned to New Zealand on February 25 under the designation Operation Tio (OP TIO). The voyage provided a ship of opportunity to undertake science activities along the route, focusing on improving maritime safety by reducing the risk for vessels operating in the Southern Ocean and Ross Sea. Science activities were grouped on three topics:

1. measurements of sea ice, waves and atmospheric properties to support improved forecasting,
2. testing the performance of ship-based and satellite sea ice detection systems and,
3. testing the performance of navigation systems and emergency beacons at high latitudes.

https://doi.org/10.5194/essd-2025-8
Preprint. Discussion started: 17 February 2025

Open Access Earth System Science Data Discussions

The range of activities were permitted by the New Zealand Government Ministry of Foreign Affairs and Trade, which administers New Zealand's obligations under the Antarctic Treaty.

1.1 Improved forecasting of the polar ocean conditions

Accurate maritime weather forecasts in the Southern Ocean and Antarctic waters are required to decrease the risk of severe damage to ships operating in the area, with particular concern regarding collocated waves and sea ice. A key enabler to improving numerical environmental prediction and increasing the accuracy of forecasts is increasing the density of observations. Within the Ross Sea, for example, the number of atmospheric, ocean and sea ice observations are limited. Buoys and drifters are routinely deployed here each Austral summer but are transported northward and out of the area within 2-3 months.

1.2 Improved detection of sea ice

Sea ice poses a significant risk to ships at sea, and the ability to detect objects using ship sensors enables responsive routing to avoid areas of high concentration. While navigation radars have long been used as a method of detecting sea ice, the distance at which sea ice can be reliably detected is considered to be <1 nm (O'Connell, Barbara J.,2008), which tends to decrease as wave heights increase. Accordingly, during high sea states when the risk of damage from ice is greatest, the ability to detect and avoid is severely degraded. New methods for improving the sea ice detection distance involve additional processing of standard navigational radar data (such as the Rutter Ice Navigator). To date, the testing of this system at sea has been limited to qualitative studies of presence and absence of sea ice (Timothy 2015). The aim of our sea ice detection experiments using ship-based radar was to determine the distance sea ice of different sizes can be detected by the Rutter Ice Navigator post-processing software.

To enable the safe planning of routes for ships, an understanding of the sea ice over hundreds of nautical miles is required. Various national organisations provide guidance that identifies areas where sea ice concentrations are nominally greater than 15%. However, sparse ice in open ocean will present in concentrations much less than this threshold, and these pose significant risks to ships. Accordingly, in regions away from the nominal marginal sea ice limit, ships often complete passages at higher speed. An impact with a piece of sea ice in those situations could result in considerable damage, and this is especially true for ships with hull ice strengthening only at the waterline and standard hull plating above and below. In the average sea states of the Southern Ocean the actual waterline of the vessel may be outside the strengthened area, allowing for

https://doi.org/10.5194/essd-2025-8
Preprint. Discussion started: 17 February 2025

a collision between sea ice present and thin hull plating. If this is coupled with higher speeds, the risk of hull damage is considerable.

In this experiment, one of the aims was to detect pieces of ice capable of damaging a ship – approximately 3 x 3 x 3 m using space-based Synthetic Aperture Radar (SAR). During the voyage, continuous video and radar observations were made to determine the density of pieces of sea ice in open water along the ship's route. SAR images along the ship's route were also obtained by Iceye and Capella Space. If a suitable area with high density of sea ice objects was encountered, an inflatable radar reflector was to be launched along with a wave buoy. This radar reflector would assist in the calibration of the SAR processing algorithms.

1.3 Improved maritime navigation

Accurate and reliable navigation systems are critical for safe and effective maritime operations, whether employed on manned or unmanned platforms. Modern electronic navigation systems typically fuse observations from multiple sources to achieve an accurate real-time estimate of location and time, however they are often reliant on measurements of absolute position from a global navigation satellite system (GNSS) receiver to correct errors that build-up in unaided navigation algorithms.

There are four independent GNSS constellations: the United States Global Positioning System (GPS), the Russian Federation GLONASS, the European Galileo system and Chinese Beidou Navigation Satellite (BDS) system. The performance and accuracy of each system is influenced by many factors such as the orbital characteristics and the signal/modulation type in use, however it is widely accepted that due to these characteristics, the theoretical performance of each GNSS become degraded at polar latitudes (see Swaszek et al, 2018).

Throughout the voyage, an experiment named ‘LOST PENGUIN’ continuously monitored the position estimates from four receivers tuned to the civil signals of each GNSS. A fifth receiver simultaneously received signals from all constellations. The empirical position and accuracy information recorded from each receiver can be compared with navigation information from HMNZS AOTEAROA to generate insights into the use of GNSS systems at high latitudes and how commercial multi-constellation receivers may be used to improve navigation and safety-at-sea systems. To the best of the authors knowledge, this dataset is the only record of measured GNSS parameters made for a direct comparison of GNSS accuracy at high latitudes.

https://doi.org/10.5194/essd-2025-8
Preprint. Discussion started: 17 February 2025

2 Data collection methodology

The data collected during the voyage included ship-based sensors, deployed instrument platforms and satellite radar acquisitions. In addition, numerical weather and ocean prediction models were established for the voyage. These methods are described in the following subsections.

2.1 Ship-based measurements

The ship-based measurements from the voyage are categorised as radar, optical, weather and geographical (i.e. motion/location) components. A technical description of each is presented as follows.

2.1.1 Radar

Two X-band radar systems were available (Table 1). The Furuno was deployed for the voyage as a dedicated input to the Rutter Sigma s6 (RUT-01500-AA) Integrated Ice Navigator and WaMoS®II System. Sea ice targets were also collected from the Kelvin Hughes X Band Sharpeye Mark II ships navigation radar.

Table 1: Radar systems onboard the ship.

System	Specification	Setup
Furuno FAR-2107/2807	25 KW X-band radar (9.41 GHz)	Installed on the bridge top 25 m above sea surface, positioned off centre, set in short pulse mode.
Kelvin Hughes sharp eye	X-band	Permanently mounted on the mast 30m above sea surface, ships staff free to change modes as required for navigation.

2.1.2 Optical

Two optical monitoring systems were installed for the voyage (Table 2, Figure 1).

The SnapIT camera is a marinised optical monitoring solution designed for fisheries research. The 1/3”4 megapixel HDR sensor (1920x1080) is optimised for dynamic image processing under high and low light with auto gain, white-balance, and exposure. The camera was connected via CAT5e ethernet cable to a SnapIT AIHub for data processing to an internal 1TB drive (SSD), with external data storage via hot-swappable USB drives. Time and location stamps were sourced from the ships NMEA stream.

https://doi.org/10.5194/essd-2025-8
Preprint. Discussion started: 17 February 2025

The polarising camera was a Phoenix 5.0 MP Polarisation Model (IMX250MZR/MYR), fitted with a 16 mm lens. The camera was housed in a waterproof housing and connected by Cat5e ethernet to a laptop in the bridge of the ship. Bespoke software was used to trigger image capture at 0.2 hz for a 500-frame sampling regime.

Figure 1: Snapshots showing the cotemporal field of view from the SnapIT camera (left) and the polarising camera (right).

Table 2: Optical systems onboard the ship.

System	Specification	Setup
SnapIT camera	FOV after lens correction 72, 43, 80 deg (horizontal, vertical, diagonal)	Mounted on starboard bridge top, 25 m elevation, 13.5 m starboard, 15FPS sampling rate.
Polarising camera	FOV 25 deg	Mounted on the central bridge top and pointed to starboard, 25 m elevation.

2.1.3 Weather

The weather monitoring systems onboard the ship are listed in Table 3.

Table 3: Weather monitoring systems onboard the ship.

System	Specification	Setup
Anemometer	Observant OIC - 118	34.6 m elevation, recording at 1 hz.
Humidity and temperature	Observant OMC - 406	28 m elevation, recording at 1 hz.
Barometric pressure	Observant OMC - 506	27 m elevation, recording at 1 hz.

https://doi.org/10.5194/essd-2025-8
Preprint. Discussion started: 17 February 2025

2.1.4 Geographical

Navigation data was collected by two independent systems during the voyage, as described in this section.

Ship navigation system

HMNZS AOTEAROA is fitted with a modern digital navigation system comprising of two forward and aft redundant iXblue Marins M3 fibre-optic inertial measurement units (IMU), feeding a Naval Data Distribution System (NAVDDS) running the iXblue NETANS software. NETANS combines inertial measurements with through-water speed from an EM-LOG, and absolute location from two SAAB R5 multi-constellation global navigation satellite system (GNSS) receivers to produce a fused navigation solution which is used throughout the ship. Messages from the NAVDDS to sensors and subsystems are typically delivered as NMEA sentences over an IP network.

With the exception of the LOST PENGUIN experiment, all data collected by the various ship sensors (Kelvin Huges, Furuno radars, etc.) which include navigation information, has been derived from the primary NAVDDS navigation source. i.e. All navigation data collected and described in this paper has been sourced from the ships primary navigation system. Collected data is therefore both location and time aligned to the position of the ship as observed by the navigation officers.

A map showing the ship position and speed during OP TIO is presented in Figure 2.

https://doi.org/10.5194/essd-2025-8
Preprint. Discussion started: 17 February 2025

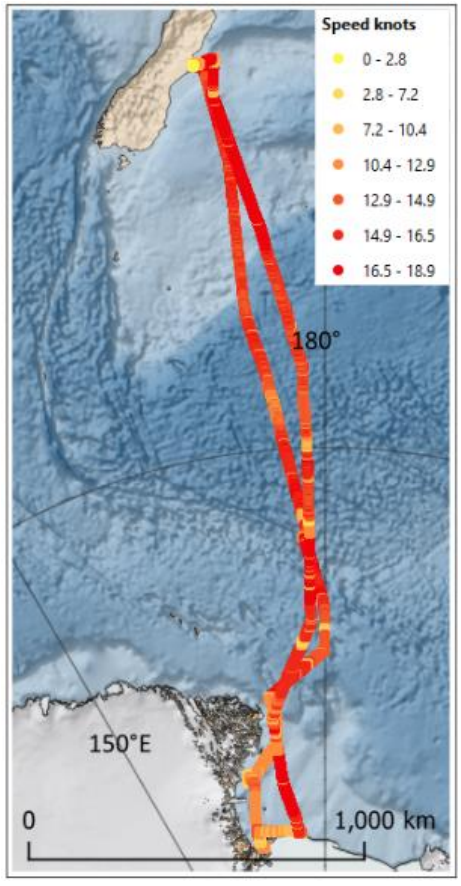

Figure 2: Position and speed of the HMNZS AOTEAROA during OP TIO.

Ship motion system

The IXBlue Marins M3 fibre optic gyros as described above also output measurements of ship motion. The IXBlue Marins M3 have a heading accuracy of 0.1° and a pitch/roll accuracy of 0.01°, with outputs as specified in Table 4.

https://doi.org/10.5194/essd-2025-8
Preprint. Discussion started: 17 February 2025

Table 4: Ship-specific parameters available for the voyage.

Parameter	Statistic per 10-minute sample
Latitude	observed at start
Longitude	observed at start
Pitch (deg)	significant, single amplitude
Roll (deg)	significant, single amplitude
Heave (m)	significant, double amplitude

LOST PENGUIN GNSS Experiment

The LOST PENGUIN experiment as depicted in Figure 3 consists of five independent uBlox ZED-F9P receivers connected to a common GNSS antenna via a passive RF splitter. This topology ensures that all receivers receive identical RF and are not biassed by using different antennas in different positions. The Tallysman VSP6037L full-band GNSS antenna incorporates an embedded low noise amplifier (LNA) to raise the signal power in the antenna. This is powered by a 5V supply from the first ZED-F9P receiver via a DC-pass channel in the GPS610 splitter. The five remaining splits in the GPS610 are DC blocked with a 200-ohm load to allow the remaining F9P receivers to believe that an antenna is connected. The sixth (unused) channel of the GPS610 splitter is terminated with a 50-ohm load to prevent return losses from mismatched splitting.

Each uBlox ZED-F9P receiver is powered from a USB 2.0 hub which provides data connectivity to an Intel NUC mini-PC to record the GNSS information onto an external USB solid state disk (SSD). When connected via USB, the ZED-F9P enumerates in the host as a virtual COM port. This allows bidirectional communication for configuration of the device and obtaining measurements.

The uBlox ZED-F9P can stream data over the USB interface in multiple wire formats, such as NMEA 0183 and uBlox Binary eXchange (UBX). Due to the compact and concise nature of UBX, data collected during the LOST PENGUIN experiment has been collected in this format. Data from each ZED-F9P receiver is streamed to the Intel NUC and saved to disk in this binary format. The data has been chunked into 10MB files in case of corruption. Full details of the UBX format and the process for recombination are given in the following section.

https://doi.org/10.5194/essd-2025-8
Preprint. Discussion started: 17 February 2025

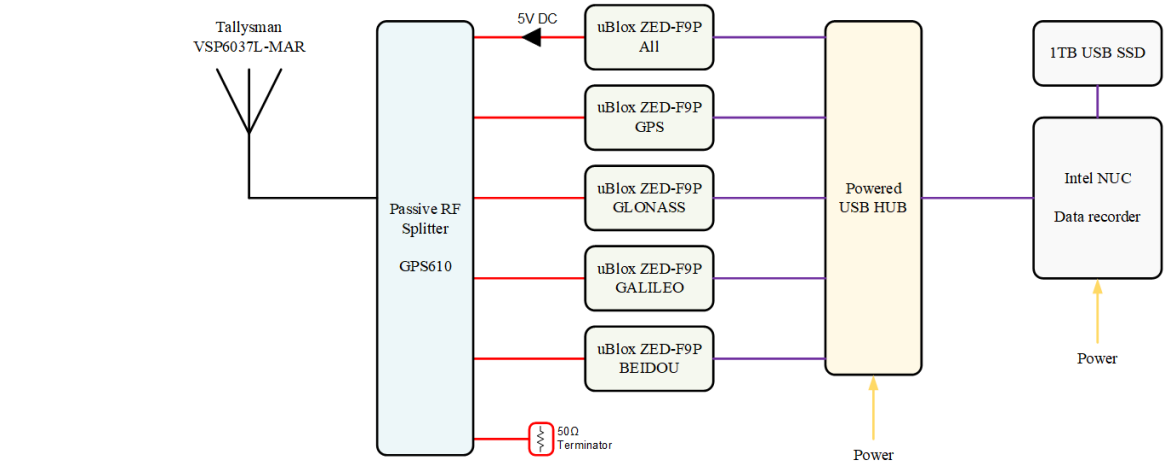

Figure 3: Data flow diagram for the LOST PENGUIN GNSS experiment.

2.2 Deployed sensors

Stand-alone platforms with a variety of sensors were deployed throughout the voyage, with the intention of providing time series data collection in the Ross Sea after the ship had returned to New Zealand. In addition, profiles of water temperature were also collected during the voyage using Expendable Bathythermograph (XBT) profilers. The location of these observations is shown Figure 2.4, with further detail provided in the following subsections.

2.2.1 Wave buoys

Two types of wave buoys were deployed, each telemetering wave spectra and wave statistics via satellite communications.

Sofar spotter buoy

Free floating Sofar Spotter wave buoys (https://www.sofarocean.com/products/spotter) were temporarily deployed to support the radar ice detection experiments as well as 15 units being released for long monitoring within the Ross Sea and Southern Ocean. These instruments were set to sample at hourly intervals and transmit directional spectral estimates in near real time via the Iridium satellite network. The message payload consists of time, position, significant wave height, peak wave period, mean direction at peak energy, peak directional spread, mean wave period, mean wave direction and mean directional wave spread. See Raghukumar, et al, (2019) for the wave data processing details. In addition, the SOFAR buoys report barometric pressure, sea surface temperature and an estimate of the surface wind speed based on the high frequency wave spectrum.

Scripps wave buoys

Four free floating wave buoys produced by the Scripps Institute of Oceanography were released into the Ross Sea, however only two were functional. The Scripps wave buoy program is described by Otero et al (2020).

https://doi.org/10.5194/essd-2025-8
Preprint. Discussion started: 17 February 2025

2.2.2 Global Drifter Program

The NOAA Global Drifter Program originated in February 1979 as part of the TOGA/Equatorial Pacific Ocean Circulation Experiment (EPOCS), with the first large-scale deployment in 1988 to map the tropical Pacific Ocean's surface circulation. The drifter program uses several different types of drifters, during OP TIO, a total of 10 Surface Velocity Program (SVP) drifters with barometers were deployed.

2.2.3 ARGO floats

ARGO (ARGO, 2022) is an international program to measure key ocean properties using free-drifting profiling floats. At present there are more than 3500 instruments deployed globally, mostly focussed on measuring the temperature and salinity of the upper 2000 m of the ocean, but with new sensors being deployed for bio-geo parameters as well as the deeper ocean regions (including the hadal zone). All data is publicly available in near real-time with automated QC, and in a six-month delayed mode following a more detailed QC. ARGO floats (WMO ID 7900930 and 7900931) were deployed at two locations within the Ross Sea (72 S, 173 E and 75 S 172 E; Figure 4).

2.2.4 XBT

XBTs provide one of the simplest and most cost-efficient solutions for frequently obtaining temperature profiles of the upper ocean while a ship is underway. The XBT contains a precision thermistor located in the nose of the probe, which is converted to temperature. The depth is computed empirically as a function of the time-since-water-contact using a well-established fall rate equation. HMNZS AOTEAROA is fitted with a Sippican Mark 21 XBT launcher system, and some 85 T-4 XBT probes were launched during the voyage (Figure 2.4). The T-4 probes have a maximum depth of 460 m and are therefore able to sample much of the water column in the margins of the Ross Sea. Note the rated temperature accuracy of the T-4 units is only +/- 0.1 deg C, which is suitable for general characterisation of the water properties in Antarctic regions (e.g. Russo, et al, 1999).

https://doi.org/10.5194/essd-2025-8
Preprint. Discussion started: 17 February 2025

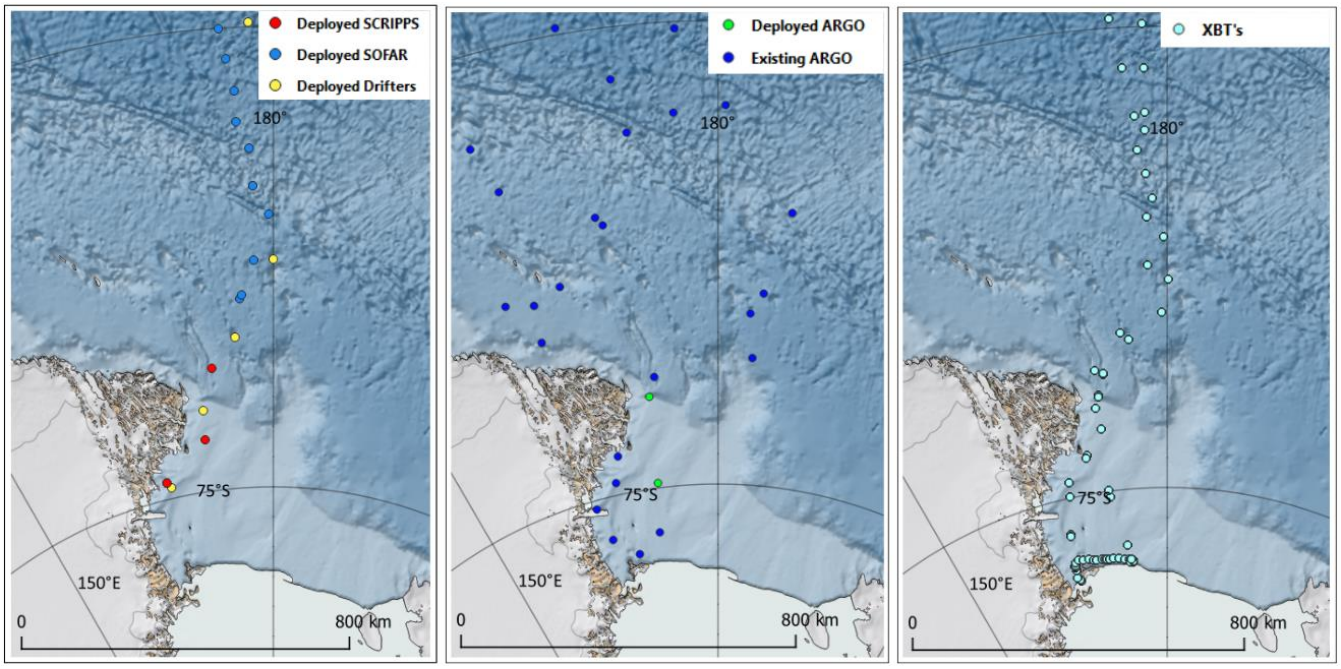

Figure 4: **Map showing all the OP TIO deployed sensors, south of 60 latitude. Left map shows Scripps wave buoys (red), Sofar wave buoys (blue) and NOAA Global Drifters (yellow). Centre map shows the ARGO floats (green) along with the existing ARGO floats at the time. Right map shows the location of the XBT profiles south of 60 latitude.**

2.3 Satellite remote-sensed data

For the Ross Sea region during February 2022, remote-sensed data from the following sources have been subset and archived to facilitate analysis with other cotemporal and collocated data:

- Quickscat (https://manati.star.nesdis.noaa.gov/datasets/QuikSCATData.php)
- Altimeter (https://manati.star.nesdis.noaa.gov/datasets/SGWHData.php)
- Daily MODIS SST (https://podaac.jpl.nasa.gov/dataset/MODIS_AQUA_L3_SST_MID-IR_DAILY_4KM_NIGHTTIME_V2019.0)
- Synthetic Aperture Radar (SAR) images were available from three sources.
- Sentinel-1 - routine acquisitions in the Ross Sea.
- Capella Space - 23 targeted acquisitions.

ICEYE - 5 targeted acquisitions funded by European Space Agency (ESA) under the Third Party Mission (TPM) scheme.

Polygons showing the location and extent of the SAR collects are shown on Figure 5.

https://doi.org/10.5194/essd-2025-8
Preprint. Discussion started: 17 February 2025

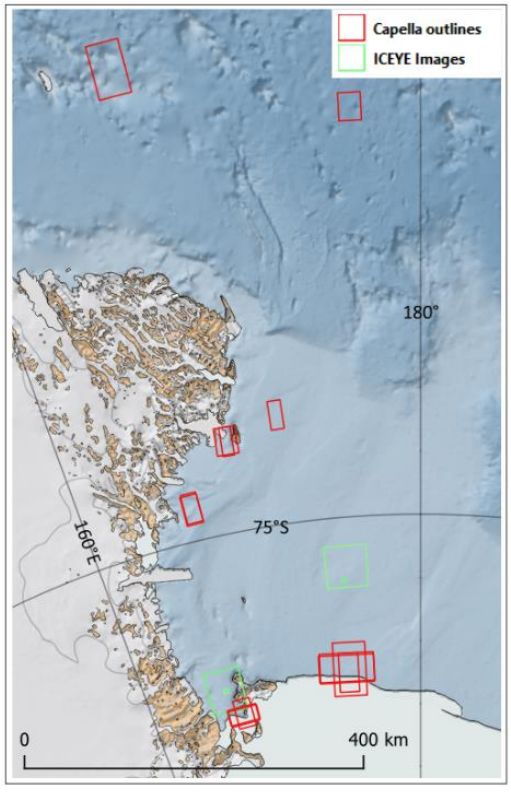

Figure 5: Polygons showing the image areas from satellite SAR collections by ICEYE and Capella.

2.4 Wave model data

A regional wave forecast model was established for the Ross Sea, and the nowcast fields (waves and winds) were archived for the month of February 2022. For regions south of 60, a SWAN spectral wave model was established, with spatial resolution of 5 km and atmospheric and sea ice boundary conditions sourced from the d_3 (2.67 km resolution) run of the operational AMPS forecasting service (www2.mmm.ucar.edu/rt/amps/). The model was nested within a global WW3 model of 0.5 degree resolution that was forced with GFS winds. The Ross Sea model was run at 6 hourly cycles, with nowcasts collated to provide hourly wave data throughout the Ross Sea. Archived files include the standard wave spectral estimates in a gridded format. See Figure 6 showing daily snapshots of significant wave height over the domain.

https://doi.org/10.5194/essd-2025-8
Preprint. Discussion started: 17 February 2025

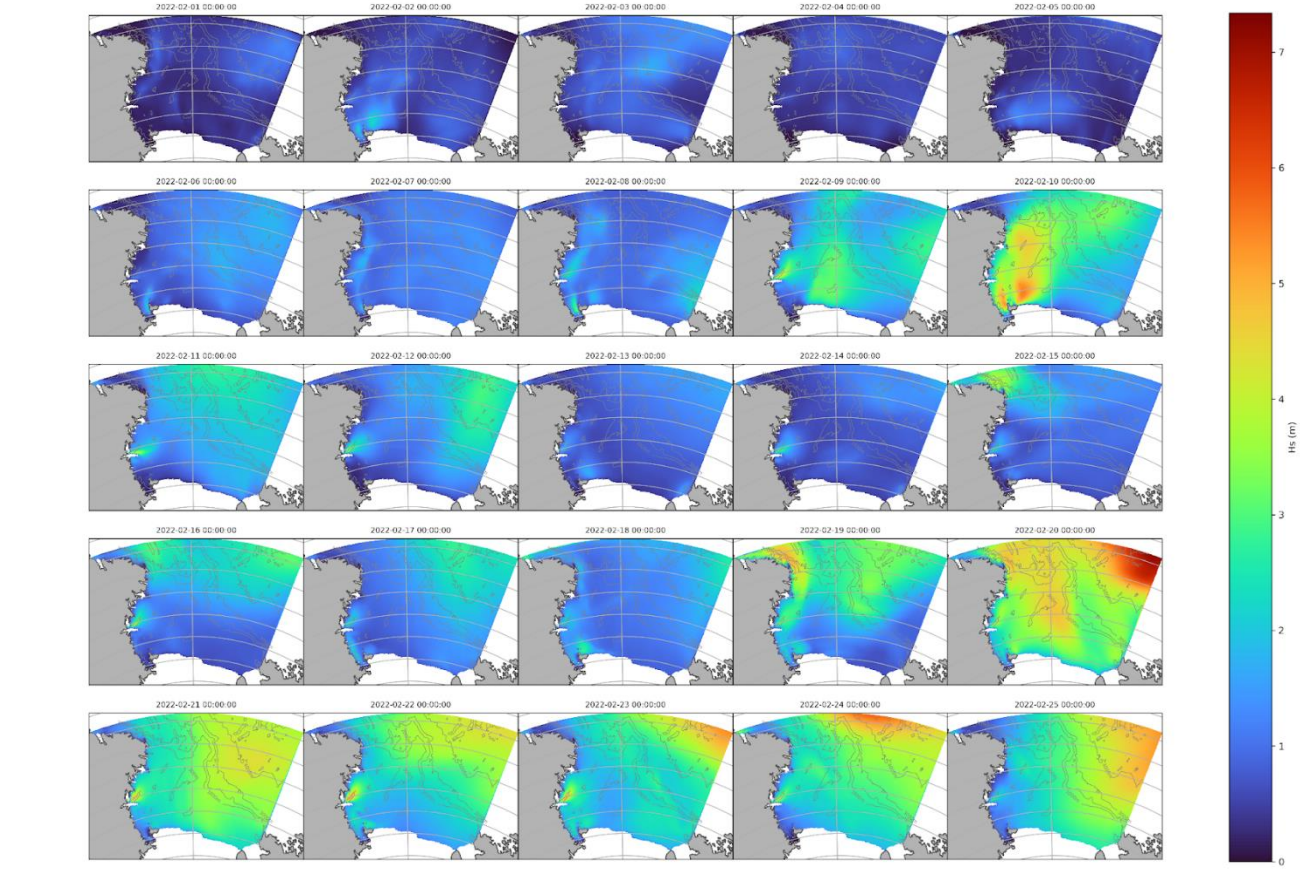

Figure 6: Daily snapshots of the nowcast significant wave heights in the Ross Sea during February 2022.

3 Data processing

The data processing methodology is outlined in this section. All files were converted to an xarray-compatible format and registered within a cloud database (oceanum.io) for user subsetting and access - see Section 4 for data access details. The data are also available in native formats from the xx repository.

3.1 Weather parameters

The ship weather observations were converted to 10-minute mean values and assigned a position based on the start of each 10-minute period. For wind, a vector average was calculated, and no adjustment for elevation was imposed.

https://doi.org/10.5194/essd-2025-8
Preprint. Discussion started: 17 February 2025


Open Access Earth System Science Data Discussions

3.2 Waves and currents by radar

Estimates of the directional sea state and surface currents in the vicinity of the ship were made using the WaMoS-II software post processing of the Furuno radar (see Reichert et al., 1999). An operational description of WaMoS is provided by Derkani et at (2021), along with a discussion of the system limitations. For OP TIO, real time observations of the wind speed and direction, ship position and water depth were ingested into the software. A sensing box of 3.2 km x 3.2 km (512 x 512 pixels) was established on the starboard and forward quarter, with a time averaging of 2 seconds applied. Note in the presence of sea ice, measurements of wave height and period cannot be reliably estimated. For every vessel installation, a calibration is required to convert the reflected radar signal strength into a significant wave height value. For OP TIO, collocated / cotemporal significant wave heights from the nowcast of a 0.5 degree WW3 global wave forecast model were used in a calibration of the system by the manufacturer. This was performed over the open ocean section of the voyage from New Zealand to 60S, return.

3.3 Ice detection by radar

Two radar methods were used to detect sea ice in the vicinity of the ship:

- the Rutter Ice Navigator application SeaView using default settings was used to detect sea ice, and
- the Kelvin Hughes Shape Eye Enhanced Target Detection module.

3.4 Ice detection by optical

A method was developed to extract the ice floes present in the video footage recorded using the SnapIT camera as georeferenced polygons. The video was first subsampled to a frequency of 1Hz and each remaining image orthorectified and corrected for ship-motion. For each image, floe locations were estimated by first identifying ice pixels using a threshold and then grouping them into coherent structures following an approach similar to Zhang and Skjetne (2014). The final ice floe polygons were extracted using a machine learning-based segmentation approach.

3.5 Geographical and vessel motion

A 10-minute time series representing statistics of the logged vessel parameters throughout the voyage was created. Time datum is UTC for the start of each 10-minute sampling period.

3.5 XBT

The XBT data were logged with a computer time datum, which was converted to UTC and renamed in the *.edf files. Also, the time lag from probe release to water contact was corrected to ensure the first wet reading was 0.6472 m below sea surface.

https://doi.org/10.5194/essd-2025-8
Preprint. Discussion started: 17 February 2025

4 Data availability and access

The complete set of OP TIO data (Garrett et al, 2024), as described in this paper, can be accessed from https://oceanum.io/. A sign-in is required, but the service is open, and the data are available under a (CC BY 4.0) licence. Once logged in to the oceanum.io portal, users should search for 'optio' to list and then access the data files in the desired format. The data is also available at Marine Data Archives (https://doi.org/10.14284/666), minus the optical and SAR files due to size, however the SAR image polygons are provided. We recommend that users apply the subsetting function in oceanum.io to extract the portions of the optical and SAR data as required.

5 Example results

The weather conditions throughout the voyage were relatively benign for the Southern Ocean. In the open ocean the significant wave heights reached only 5.7 m and the highest 10-minute mean wind speed was 31 m/s. As this was a resupply operation to McMurdo Station, the ship's crew actively optimised the course to ensure the safety of the upper deck cargo.

The sea ice conditions encountered during the voyage were also benign, and at the time the ice-covered area during February 2022 was the 4th lowest recorded since 1979. On the voyage south HMNZS AOTEAROA entered the Ross Sea near Scott Island (67 22 S, 179 54 E) and could have transited to McMurdo Sound via open water. However, to enable crew training in sea ice, the ship altered course toward Cape Adare and Terra Nova Bay to engage with sea ice. In the latter location, the region was used for testing the performance of Rutter Sigma 6 Ice Navigator. On the return voyage the ship encountered 10/10th sea ice concentration on the western side of Ross Island for approximately 50 nm.

The following subsections provide examples from the OP TIO datasets.

5.1 Temperature profiles along latitude and longitude transects

Two XBT transects from the voyage are presented in Figures 7 and 8. The first shows temperature profiles along the front of the Ross Ice Shelf, suggesting a complex flow structure adjacent to the ice and in the vicinity of Ross Island. Temperature profiles from south (77S) to north (60S) are presented in Figure 8, showing the clear latitudinal gradient caused by the Ross Sea thermohaline circulation regime.

5.2 Measured and modelled significant wave heights in the Ross Sea

We present a comparison of the measured and modelled significant wave heights over two periods when the vessel was in open water in the southern Ross Sea (Fig. 9). In this region, the sea state was observed to respond rapidly to the local wind conditions, and in general the nowcasts adequately replicate the wave conditions for operational analyses.

https://doi.org/10.5194/essd-2025-8
Preprint. Discussion started: 17 February 2025

5.3 Remote Synthetic Aperture Radar (SAR) imagery with the ship in view

A Capella SAR collect on 17/02/2022 included the ship in view, while radar detection experiments were underway (Fig. 10). The measured weather conditions were a significant wave height of 3.1 m at 6 s peak period, with 10-minute mean wind speed of 24 knots from 245 degT.

5.4 Mosaic of optical images showing ice concentrations

A mosaic of the georectified optical images from 09/02/2022 is presented in Figure 11. Here, the ship was transiting through an area of 10/10 sea ice.

5.5 Vertical accuracy of GNSS with latitude

We present in Figure 12 a scatter plot showing the vertical accuracy for each of the four GNSS receivers tested during the voyage. Here, the data are plotted for the average accuracy for each minute of latitude (nautical mile). For BeiDou and Galileo the vertical accuracy increases (becomes less accurate) from 44S to 77S. BeiDou and Galileo constellations should offer complete global coverage (Zhang et al 2019), however in this same study these two constellations were identified as having the highest global dilution of precision in the Ross Sea area. For GPS vertical accuracy remains similar, which is inconsistent with theoretical predictions based on the satellite orbital inclination (e.g. Swaszek et al, 2018) where a degradation in the horizontal and vertical accuracy is expected in high latitudes (i.e. above 60-70 deg). We propose that the increased number of satellites in the GPS network since 2018 has meant an improvement in accuracy. For Glonass the vertical accuracy decreases with increasing latitude

https://doi.org/10.5194/essd-2025-8
Preprint. Discussion started: 17 February 2025

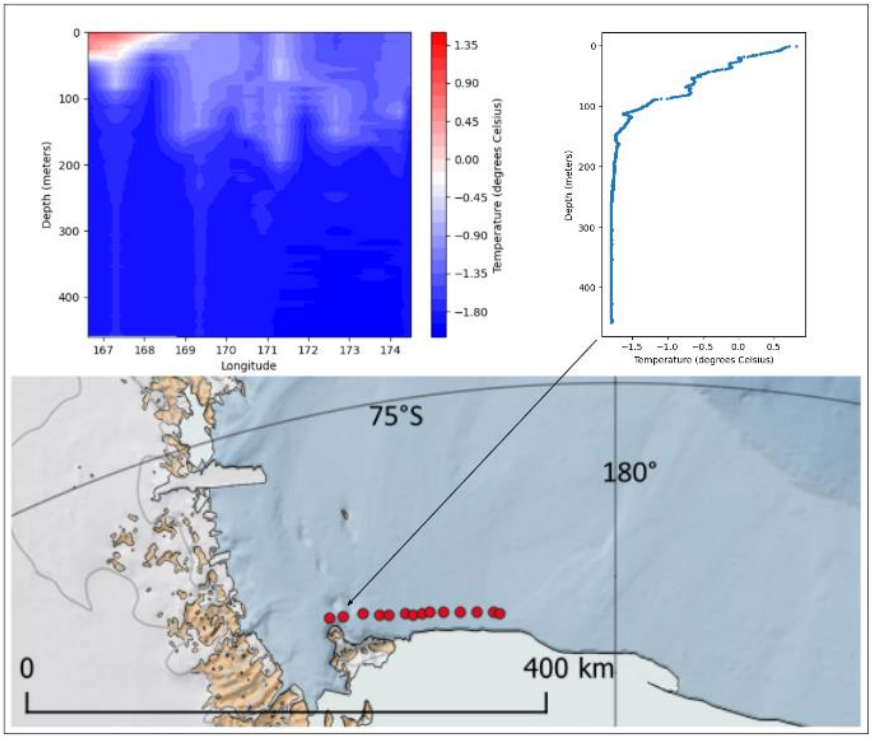

Figure 7: XBT temperature profiles by longitude from Ross Island and across the front of the Ross Ice Shelf.

340

https://doi.org/10.5194/essd-2025-8
Preprint. Discussion started: 17 February 2025

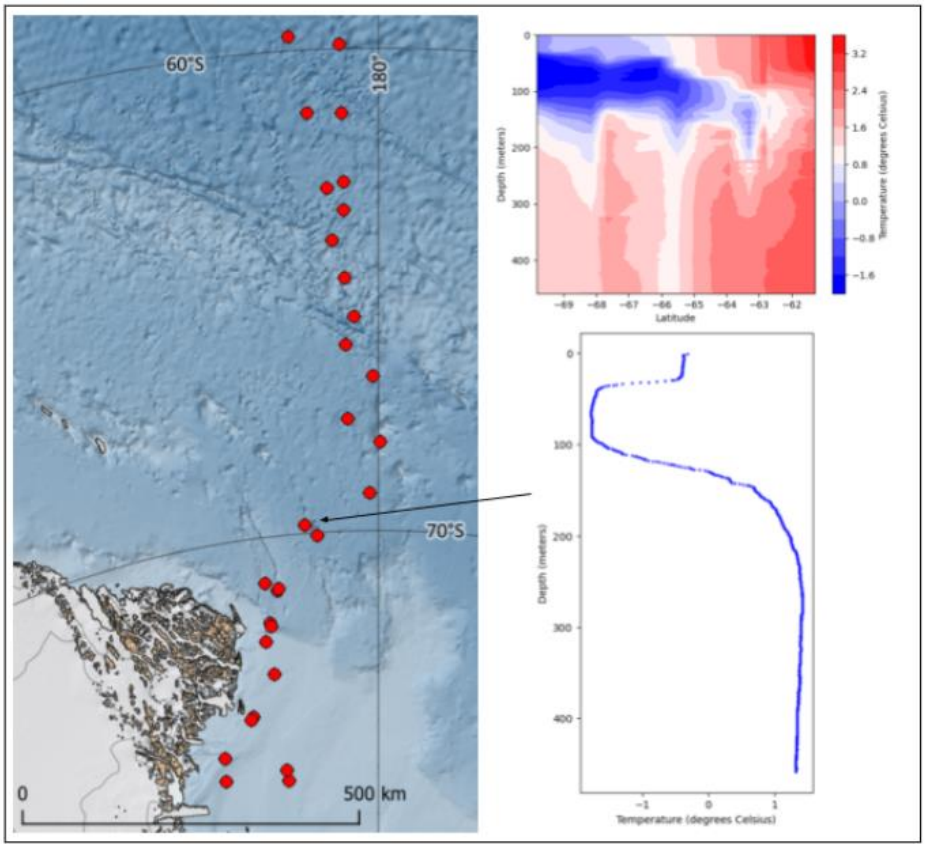

Figure 8: XBT temperature profiles by latitude from 77 to 60 S.

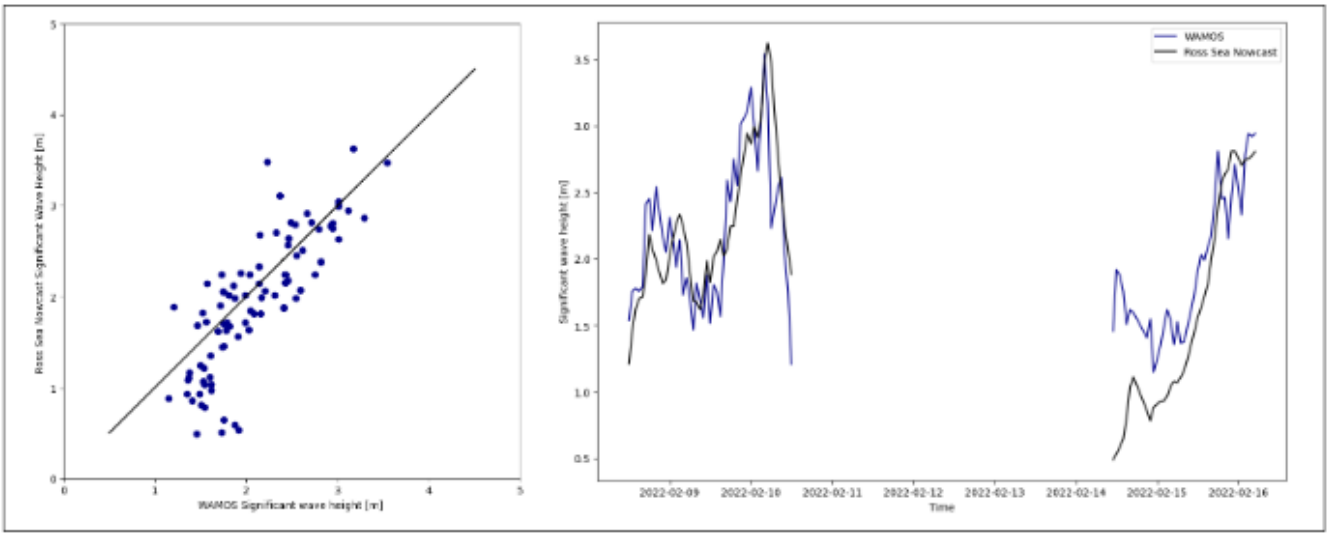

345 **Figure 9: Scatter plot of measured vs modelled significant wave heights (left) and a time timeseries of the same (right).**

https://doi.org/10.5194/essd-2025-8
Preprint. Discussion started: 17 February 2025

Figure 10: Capella Synthetic Aperture Radar image from 17/02/2022, showing the HMNZS AOTEAROA (red circle) and various ice features.

350

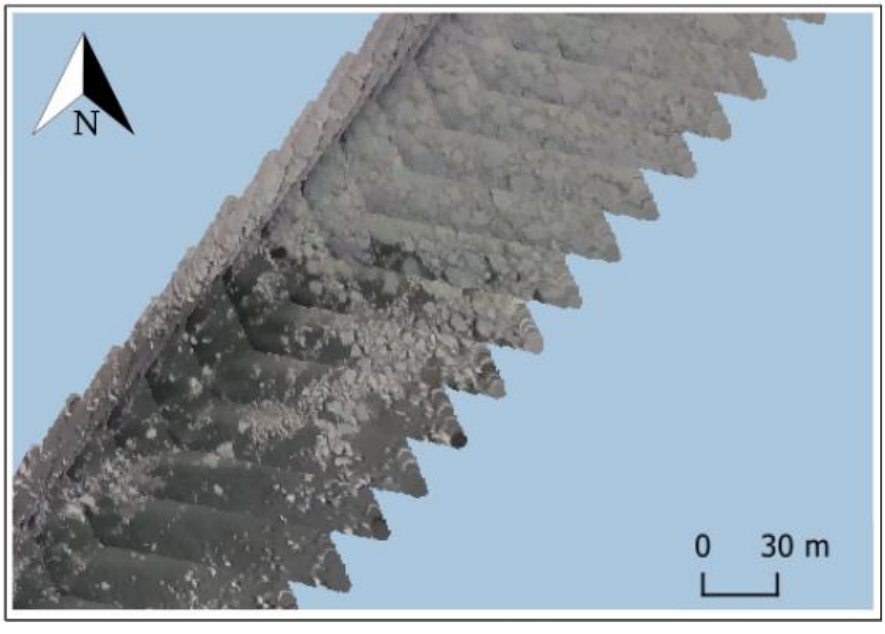

Figure 11: Mosaic of georectified optical images showing a transition to 10/10 sea ice cover.

https://doi.org/10.5194/essd-2025-8
Preprint. Discussion started: 17 February 2025

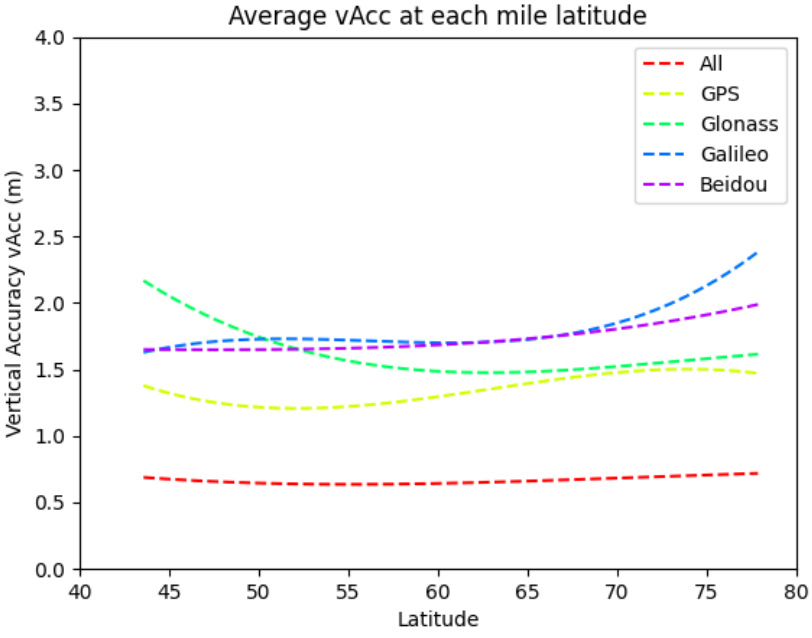

355 **Figure 12: Scatter plot showing the vertical accuracy vs latitude for each of the four GNSS receivers.**

6 Summary

The paper presents a range of open data that was collected from the HMNZS AOTEAROA during the maiden resupply voyage to McMurdo Sound, Antarctica. Experiments were conducted to support studies that are focussed on improving maritime safety in the Southern Ocean. The science program included 21 free floating wave buoys, 10 Global Drifters, 2
360 Argo Floats and 85 expendable bathythermograph profilers. Measurements of meteorological, oceanographic, and sea ice characteristics were captured from onboard the ship and augmented with satellite-based synthetic aperture radar collects and high-resolution wave modelling. An aligned experiment was also undertaken to assess the performance of Global Navigation Satellite Systems at high latitudes.

7 Author contribution

365 Garrett, McComb and Harris undertook the planning and execution of the experiments. McComb and Garrett undertook the writing of this paper, while Crabtree provided visualisation and data curation.

https://doi.org/10.5194/essd-2025-8
Preprint. Discussion started: 17 February 2025

8 Competing interests

The authors declare that they have no conflict of interest.

References

Argo (2022). Argo float data and metadata from Global Data Assembly Centre (Argo GDAC). SEANOE. https://doi.org/10.17882/42182.

Derkani, M. H., Alberello, A., Nelli, F., Bennetts, L. G., Hessner, K. G., MacHutchon, K., Reichert, K., Aouf, L., Khan, S., and Toffoli, A.: Wind, waves, and surface currents in the Southern Ocean: observations from the Antarctic Circumnavigation Expedition, Earth Syst. Sci. Data, 13, 1189–1209, https://doi.org/10.5194/essd-13-1189-2021, 2021.

Carr, Kevin, Robert Greer, Marvin B. May, and Scott Gift. "Navy testing of the iXBlue MARINS fiber optic gyroscope (FOG) inertial navigation system (INS)." In *2014 IEEE/ION Position, Location and Navigation Symposium-PLANS 2014*, pp. 1392-1408. IEEE, 2014.

Garrett, S., McComb, P., Harris, J.; Crabtree, U. Science data collection by the New Zealand Defence Force during the 2022 Antarctic Resupply Mission. Marine Data Archive. https://doi.org/10.14284/666, 2024.

Reichert, K., Hessner, K., Nieto Borge, J. C., and Dittmer, J.: WaMoS-II: A radar-based wave and current monitoring system, in: The Ninth International Offshore and Polar Engineering Conference (ISOPE), International Society of Offshore and Polar Engineers, Brest, France, May 1999, ID: ISOPE-I-99-246, 1999.

O'Connell, Barbara J. "Marine Radar for Improved Ice Detection." Paper presented at the SNAME 8th International Conference and Exhibition on Performance of Ships and Structures in Ice, Banff, Alberta, Canada, July 2008. DOI: https://doi.org/10.5957/ICETECH-2008-136.

Timothy, M., & Girton, R. (2015). Evaluation of Rutter Sigma S6 Ice Navigation Radar on USCGC Healy during Arctic Shield 2014 ii. Retrieved from https://apps.dtic.mil/sti/pdfs/ADA615477.pdf.

Swaszek, Peter F., Hartnett, Richard J., Seals, Kelly C., Siciliano, Joseph D., Swaszek, Rebecca M. A., "Limits on GNSS Performance at High Latitudes," Proceedings of the 2018 International Technical Meeting of The Institute of Navigation, Reston, Virginia, January 2018, pp. 160-176.

https://doi.org/10.33012/2018.15549.

u-blox F9 HPG 1.32 Interface Description. 02-May-2022 Describes the UBX wire format. Available online: https://content.u-blox.com/sites/default/files/documents/u-blox-F9-HPG-1.32_InterfaceDescription_UBX-22008968.pdf

Otero M, Terrill E, Merrifield S, Ardhuin F (2020). Scripps Institution of Oceanography drifting wave buoy array in sea ice, 2018. SEANOE. https://doi.org/10.17882/72284.

Pan, L., Zhang, X., Li, X., Li, X., Lu, C., Liu, J., & Wang, Q. (2019). Satellite availability and point positioning accuracy evaluation on a global scale for integration of GPS, GLONASS, BeiDou and Galileo. Advances in Space Research, 63(9), 2696–2710. https://doi.org/10.1016/j.asr.2017.07.029.

Raghukumar, K., G. Chang, F. Spada, C. Jones, T. Janssen, and A. Gans, 2019: Performance Characteristics of "Spotter," a Newly Developed Real-Time Wave Measurement Buoy. J. Atmos. Oceanic Technol., 36, 1127–1141, https://doi.org/10.1175/JTECH-D-18-0151.1.

Zhang, Q. and Skjetne, R., 2014: Image processing for identification of sea-ice floes and the floe size distributions. IEEE Transactions on geoscience and remote sensing, 53(5), 2913-2924.

Russo, A., Artegiani, A., Budillon, G., Paschini, E., Spezie, G. (1999). Upper Ocean Thermal Structure and Fronts Between New Zealand and the Ross Sea (Austral Summer 1994–1995 and 1995–1996). In: Spezie, G., Manzella, G.M.R. (eds) Oceanography of the Ross Sea Antarctica. Springer, Milano. https://doi.org/10.1007/978-88-470-2250-8_5.